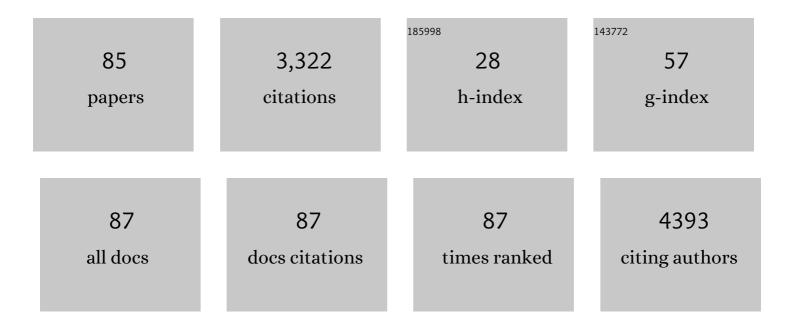
## Aaron Stein

List of Publications by Year in descending order

Source: https://exaly.com/author-pdf/9299976/publications.pdf Version: 2024-02-01



#	Article	IF	CITATIONS
1	Broadband achromatic dielectric metalenses. Light: Science and Applications, 2018, 7, 85.	7.7	449
2	Controlling propagation and coupling of waveguide modes using phase-gradient metasurfaces. Nature Nanotechnology, 2017, 12, 675-683.	15.6	323
3	Thermal ground-state ordering and elementary excitations in artificial magnetic square ice. Nature Physics, 2011, 7, 75-79.	6.5	297
4	Dielectric metasurfaces for complete and independent control of the optical amplitude and phase. Light: Science and Applications, 2019, 8, 92.	7.7	278
5	Hot Carrier Electroluminescence from a Single Carbon Nanotube. Nano Letters, 2004, 4, 1063-1066.	4.5	162
6	High-density waveguide superlattices with low crosstalk. Nature Communications, 2015, 6, 7027.	5.8	116
7	Single-element elliptical hard x-ray micro-optics. Optics Express, 2003, 11, 919.	1.7	106
8	Optical conductivity-based ultrasensitive mid-infrared biosensing on a hybrid metasurface. Light: Science and Applications, 2018, 7, 67.	7.7	98
9	Aberration-Corrected Electron Beam Lithography at the One Nanometer Length Scale. Nano Letters, 2017, 17, 4562-4567.	4.5	80
10	Indium Tin Oxide Broadband Metasurface Absorber. ACS Photonics, 2018, 5, 3526-3533.	3.2	78
11	Interaction modifiers in artificial spin ices. Nature Physics, 2018, 14, 375-379.	6.5	76
12	High-strength magnetically switchable plasmonic nanorods assembled from a binary nanocrystal mixture. Nature Nanotechnology, 2017, 12, 228-232.	15.6	75
13	Correlated Perovskites as a New Platform for Superâ€Broadbandâ€Tunable Photonics. Advanced Materials, 2016, 28, 9117-9125.	11.1	72
14	A 60 Gb/s MDM-WDM Si photonic link with < 07 dB power penalty per channel. Optics Express, 2014, 22, 18543.	1.7	69
15	Frustration and thermalization in an artificial magnetic quasicrystal. Nature Physics, 2018, 14, 309-314.	6.5	62
16	Measurement of hard x-ray lens wavefront aberrations using phase retrieval. Applied Physics Letters, 2011, 98, 111108.	1.5	50
17	Nanofabrication on unconventional substrates using transferred hard masks. Scientific Reports, 2015, 5, 7802.	1.6	50
18	Hybrid Metasurface-Based Mid-Infrared Biosensor for Simultaneous Quantification and Identification of Monolayer Protein. ACS Photonics, 2019, 6, 501-509.	3.2	47

#	Article	IF	CITATIONS
19	Generation of Ensembles of Individually Resolvable Nitrogen Vacancies Using Nanometer-Scale Apertures in Ultrahigh-Aspect Ratio Planar Implantation Masks. Nano Letters, 2015, 15, 1751-1758.	4.5	44
20	Gaussian processes for autonomous data acquisition at large-scale synchrotron and neutron facilities. Nature Reviews Physics, 2021, 3, 685-697.	11.9	44
21	Real and effective thermal equilibrium in artificial square spin ices. Physical Review B, 2013, 87, .	1.1	40
22	Cascade Pumping of 1.9–3.3 μ4m Type-I Quantum Well GaSb-Based Diode Lasers. IEEE Journal of Selected Topics in Quantum Electronics, 2017, 23, 1-8.	1.9	40
23	Patterning Si at the 1 nm Length Scale with Aberration orrected Electronâ€Beam Lithography: Tuning of Plasmonic Properties by Design. Advanced Functional Materials, 2019, 29, 1903429.	7.8	39
24	Ultrahigh Elastic Strain Energy Storage in Metal-Oxide-Infiltrated Patterned Hybrid Polymer Nanocomposites. Nano Letters, 2017, 17, 7416-7423.	4.5	38
25	Direct fabrication of high aspect-ratio metal oxide nanopatterns via sequential infiltration synthesis in lithographically defined SU-8 templates. Journal of Vacuum Science and Technology B:Nanotechnology and Microelectronics, 2015, 33, 06F201.	0.6	37
26	Nanoimprinted Chiral Plasmonic Substrates with Three-Dimensional Nanostructures. Nano Letters, 2018, 18, 7389-7394.	4.5	36
27	Electrical and structural properties of ZnO synthesized via infiltration of lithographically defined polymer templates. Applied Physics Letters, 2015, 107, .	1.5	31
28	Advancing next generation nanolithography with infiltration synthesis of hybrid nanocomposite resists. Journal of Materials Chemistry C, 2019, 7, 8803-8812.	2.7	30
29	Fabrication of silicon kinoform lenses for hard x-ray focusing by electron beam lithography and deep reactive ion etching. Journal of Vacuum Science & Technology B, 2008, 26, 122.	1.3	25
30	Guiding light in bent waveguide superlattices with low crosstalk. Optica, 2019, 6, 585.	4.8	25
31	Thermal transitions in nano-patterned XY-magnets. Applied Physics Letters, 2014, 105, 042409.	1.5	23
32	Local structure of human hair spatially resolved by sub-micron X-ray beam. Scientific Reports, 2015, 5, 17347.	1.6	23
33	Magnetotransport properties of <mml:math xmlns:mml="http://www.w3.org/1998/Math/MathML"&gt; <mml:msub> <mml:mi>MoP</mml:mi> <mml:mn>2Physical Review B, 2017, 96, .</mml:mn></mml:msub></mml:math 	l:m <b>a.</b> x <td>ml<b>:ា2ន</b>ub&gt;</td>	ml <b>:ា2ន</b> ub>
34	One-dimensional hard x-ray field retrieval using a moveable structure. Optics Express, 2010, 18, 18374.	1.7	21
35	Si^+-implanted Si-wire waveguide photodetectors for the mid-infrared. Optics Express, 2014, 22, 27415.	1.7	21
36	Chemo- and Thermomechanically Configurable 3D Optical Metamaterials Constructed from Colloidal Nanocrystal Assemblies. ACS Nano, 2020, 14, 1427-1435.	7.3	20

#	Article	IF	CITATIONS
37	Linear field demagnetization of artificial magnetic square ice. Frontiers in Physics, 2013, 1, .	1.0	19
38	Extreme Carrier Depletion and Superlinear Photoconductivity in Ultrathin Parallelâ€Aligned ZnO Nanowire Array Photodetectors Fabricated by Infiltration Synthesis. Advanced Optical Materials, 2017, 5, 1700807.	3.6	17
39	Magnetic order and energy-scale hierarchy in artificial spin-ice structures. Physical Review B, 2018, 98,	1.1	16
40	3D Nanofabrication via Chemoâ€Mechanical Transformation of Nanocrystal/Bulk Heterostructures. Advanced Materials, 2018, 30, e1800233.	11.1	15
41	Spatial dependence and mitigation of radiation damage by a line-focus mini-beam. Acta Crystallographica Section D: Biological Crystallography, 2010, 66, 1287-1294.	2.5	14
42	Mitigation of X-ray damage in macromolecular crystallography by submicrometre line focusing. Acta Crystallographica Section D: Biological Crystallography, 2013, 69, 1463-1469.	2.5	14
43	Observation of the nonlinear Wood's anomaly on periodic arrays of nickel nanodimers. Physical Review B, 2018, 98, .	1.1	14
44	Metal-semiconductor-metal ion-implanted Si waveguide photodetectors for C-band operation. Optics Express, 2014, 22, 9150.	1.7	13
45	High-purity transmission of a slow light odd mode in a photonic crystal waveguide. Optics Letters, 2012, 37, 3189.	1.7	12
46	Collective magnetic dynamics in artificial spin ice probed by ac susceptibility. Physical Review B, 2020, 101, .	1.1	12
47	Defect tolerant extreme ultraviolet lithography technique. Journal of Vacuum Science and Technology B:Nanotechnology and Microelectronics, 2012, 30, .	0.6	10
48	Narrow Ridge \$lambda approx 3\$ - \$mu ext{m}\$ Cascade Diode Lasers With Output Power Above 100 mW at Room Temperature. IEEE Photonics Technology Letters, 2015, 27, 2425-2428.	1.3	10
49	Soft xâ€ray microscopy at the NSLS. Synchrotron Radiation News, 2003, 16, 11-15.	0.2	9
50	Demonstration of a hitless bypass switch using nanomechanical perturbation for high-bitrate transparent networks. Optics Express, 2010, 18, 3045.	1.7	9
51	Broadband Circular Polarizers via Coupling in 3D Plasmonic Meta-Atom Arrays. ACS Photonics, 2021, 8, 1286-1292.	3.2	9
52	Nanofabrication of doped, complex oxides. Journal of Vacuum Science and Technology B:Nanotechnology and Microelectronics, 2012, 30, 011804.	0.6	8
53	Defect-free periodic structures using extreme ultraviolet Talbot lithography in a table-top system. Journal of Vacuum Science and Technology B:Nanotechnology and Microelectronics, 2013, 31, 06F604.	0.6	7
54	External cavity cascade diode lasers tunable from 3.05 to 3.25  μm. Optical Engineering, 2017, 57, 1.	0.5	7

#	Article	IF	CITATIONS
55	Photodetectors: Extreme Carrier Depletion and Superlinear Photoconductivity in Ultrathin Parallelâ€Aligned ZnO Nanowire Array Photodetectors Fabricated by Infiltration Synthesis (Advanced) Tj ETQq1	1 037&4314	1 rgBT /Over
56	Multiple energy scales in mesospin systems: The vertex-frustrated Saint George lattice. Physical Review Materials, 2021, 5, .	0.9	6
57	Large-aperture refractive lenses for momentum-resolved spectroscopy with hard X-rays. Journal of Synchrotron Radiation, 2013, 20, 591-595.	1.0	4
58	Two-Step Narrow Ridge Cascade Diode Lasers Emitting Near \$2~mu\$ m. IEEE Photonics Technology Letters, 2017, 29, 485-488.	1.3	4
59	Single-Digit Nanometer Electron-Beam Lithography with an Aberration-Corrected Scanning Transmission Electron Microscope. Journal of Visualized Experiments, 2018, , .	0.2	4
60	Hard x-ray Fresnel prisms: properties and applications. , 2004, , .		3
61	Energy-dependent focusing properties of a kinoform Fresnel lens. , 2004, 5539, 73.		3
62	Diffraction limited 3.1514m cascade diode lasers. Semiconductor Science and Technology, 2014, 29, 115016.	1.0	3
63	Ar+-Implanted Si-Waveguide Photodiodes for Mid-Infrared Detection. Photonics, 2016, 3, 46.	0.9	3
64	High-Spectral-Contrast Symmetric Modes in Photonic Crystal Dual Nanobeam Resonators. IEEE Photonics Technology Letters, 2016, 28, 2137-2140.	1.3	3
65	Coherent amplification of X-ray scattering from meso-structures. IUCrJ, 2017, 4, 604-613.	1.0	3
66	Dual-Wavelength Y-Branch DBR Lasers With 100 mW of CW Power Near 2 μm. IEEE Photonics Technology Letters, 2020, 32, 1017-1020.	1.3	3
67	Imaging with single-dimension kinoform lenses. , 2004, , .		2
68	1â€nm Si Patterning: Patterning Si at the 1 nm Length Scale with Aberrationâ€Corrected Electronâ€Beam Lithography: Tuning of Plasmonic Properties by Design (Adv. Funct. Mater. 52/2019). Advanced Functional Materials, 2019, 29, 1970353.	7.8	2
69	Electrically pumped epitaxially regrown GaSbâ€based typeâ€l quantum well surface emitting lasers with buried highâ€indexâ€contrast photonic crystal layer Physica Status Solidi - Rapid Research Letters, 0, , 2100425.	1.2	2
70	Bending Performance of a Dense Waveguide Superlattice. , 2016, , .		2
71	Kinoform lenses: toward nanometer resolution. , 2005, 6002, 202.		1

72 High-Density Low-Crosstalk Waveguide Superlattice. , 2015, , .

1

#	Article	IF	CITATIONS
73	Scanning Soft X-ray Microscopy and Diffraction Imaging. Microscopy and Microanalysis, 2004, 10, 120-121.	0.2	0
74	Transmission electron microscopy: A linewidth measurement technique for lithography. Journal of Vacuum Science & Technology B, 2006, 24, 3077.	1.3	0
75	Near-field observation of zero index bandgaps in negative refraction photonic superlattices. , 2011, , .		0
76	Parametric oscillations and phase noise of an optomechanical air-slot photonic crystal cavity. , 2012, ,		0
77	Diffraction limited 3.15 μm cascade diode lasers. , 2014, , .		0
78	Active metasurface devices based on correlated perovskites. , 2016, , .		0
79	Kinoform lenses for high photon energies. AIP Conference Proceedings, 2019, , .	0.3	0
80	Zero phase accumulation in negative-index photonic crystal superlattices. , 2011, , .		0
81	Defect Tolerant Extreme Ultraviolet Lithography. , 2012, , .		0
82	High-purity Odd Mode Transmission in a Photonic Crystal Waveguide and Slow-light Mode Beating. , 2013, , .		0
83	Triangular nanobeam fabrication strategy for quantum photonic network realization in bulk diamond. , 2014, , .		0
84	Implantation of proximal NV clusters in diamond by lithographically defined silicon masks with 5 nm resolution. , 2014, , .		0
85	Guiding Light in Waveguide Superlattice Bends. , 2019, , .		0